Chapter 16

Chemical Solution Deposition Technique of Thin-Film Ceramic Electrolytes for Solid Oxide Fuel Cells

Mridula Biswas and Pei-Chen Su

Additional information is available at the end of the chapter

http://dx.doi.org/10.5772/66125

Abstract

Chemical solution deposition (CSD) technique is recently gaining momentum for the fabrication of electrolyte materials for solid oxide fuel cells (SOFCs) due to its cost-effectiveness, high yield, and simplicity of the process requirements. The advanced vacuum deposition techniques such as sputtering, atomic layer deposition (ALD), pulsed laser deposition (PLD), metallo-organic chemical vapor deposition (MOCVD) are lacking in scalability and cost-effectiveness. CSD technique includes a variety of approaches such as sol-gel process, chelate process, and metallo-organic decomposition. The present chapter discusses briefly about the evolution of CSD method and its subsequent entry to the field of SOFCs, various solution methods associated with different chemical compositions, film deposition techniques, chemical reactions, heat treatment strategies, nucleation and growth kinetics, associated defects, etc. Examples are cited to bring out the history dating back to the discovery of amorphous zirconia film through the successful fabrication of the crystalline fluorite-type films such as yttria-stabilized zirconia (YSZ), scandia-doped ceria (SDC), and crystalline perovskite-type films such as yttria-doped barium zirconate (BZY) and yttria-doped barium cerate (BCY), to name a few.

Keywords: chemical solution deposition, solid oxide fuel cell, ceramic electrolyte, thin films

1. Introduction

The high-temperature solid oxide fuel cells (HTSOFCs, ≥750°C) are yet to find widespread commercialization due to its high cost and short lifetime associated with its high-temperature operation. Thus, the demand for low-cost solid oxide fuel cells (SOFCs) has stimulated

research to develop low-temperature SOFCs (LTSOFCs, ≤500°C) [1]. Since the high performance of SOFCs requires high operating temperature to activate electrochemical reactions and charge transport processes, reduction in operating temperature will sacrifice performance of SOFCs. Therefore, attempts have been made to find new materials and fabrication technologies for LTSOFCs so that performance remains the same or gets enhanced. One of the main challenges in decreasing the operating temperature is the lower electrolyte conductivity, which resulted in high ohmic resistance, and deteriorates the fuel cell performance. Efforts have been made to enhance performance via reducing the thickness of ceramic electrolyte [2–8]. As the resistance of ionic charge transportation across the electrolyte obeys Ohm's law, thinner film offers less resistance to the ionic conduction and provides lower area-specific resistance. Various thin-film fabrication methods have been developed to date including vacuum-based [9–15] and non-vacuum-based methods [16–18]. Among them, chemical solution deposition (CSD) technique has been a promising technique for its high yield, versatility, and low investment cost. Moreover, the characteristic of CSD method allows easy deposition of the film over the large area up to several square meters [19]. The following paragraphs will be discussing the progress of the concept of thin film and discovery and progress of CSD method.

1.1. The concept of thin-film electrolyte and its progress

The concept of the thin-film electrolyte was first introduced with the fabrication of 400 μm thick stabilized zirconia (SZ) electrolyte in the 1960s [20]. The trend continued with the development of 30 μm thick yttria-stabilized zirconia (YSZ) electrolyte which, for the first time, successfully demonstrated the remarkable reduction of ohmic resistance from 1 to 3×10^{-3} Ω owing to minimization of the thickness of electrolyte from 1 mm to 30 μm [16]. In 1977, one electrochemical experiment, for the first time, achieved 0.91 V of open-circuit voltage (OCV) at 400°C with 0.05–1.7 μm thick calcia-stabilized zirconia (CSZ) film [10], which is a major breakthrough for LTSOFCs. With the progress in the R&D sector, Westinghouse Electric Corporation first launched cathode-supported tubular cell with 50 μm thick electrolyte, which was the first appearance of SOFC with a film electrolyte in the commercial sector [14]. All these developments were carried out with the vacuum-based methods (i.e., electrochemical vapor deposition, physical vapor deposition, chemical vapor deposition, sputtering, etc.) which lack in scalability and cost-effectiveness. As the alternative to those methods, slurry and solution-based methods were adopted. They are atmospheric or vacuum plasma spraying [21], spray pyrolysis [22], slurry coating [23, 24], and CSD [17, 18]. Although these methods are successful for micrometer thick film, the thickness of the electrolyte could not be brought down to the sub-micrometer level. With the miniaturization of SOFCs, demand for sub-micrometer thin electrolyte has been generated. CSD-based method has recently demonstrated its ability to produce films with sub-micrometer thickness.

1.2. Discovery and progress of CSD

The CSD method was introduced with the discovery of silica (SiO_2) gel from silicon alkoxide in humidified atmosphere in the middle of the nineteenth century [25]. The potential of this technique was realized with the application of single and multilayered coating of titania

(TiO_2), zirconia (ZrO_2), alumina (Al_2O_3), etc. on SiO_2 glass in the 1950s, and henceforth commercialization followed [26–28]. The development of YSZ film fabrication method started with the invention of amorphous coating of ZrO_2 film in the Central Glass and Ceramic Research Institute, India, in 1984 [17]; the Lawrence Berkeley National Laboratory took a pioneering role to develop crack-free, smooth crystalline 0.1–2 μm thin YSZ electrolyte film with sufficiently high conductivity at a temperature of 450°C [29]. Gastightness of YSZ film was demonstrated for the first time with the achievement of promising open-circuit voltage (OCV) of 0.85 V at 600°C [30]. This optimistic result casts light on the rapid progress of CSD method in the field of SOFCs. In 1912, Korea Institute of Science and Technology, South Korea, reported the fabrication of a dense and gastight bilayer electrolyte of YSZ/gadolinia-doped ceria (GDC) with thickness of 100/400 nm. The success of this process was established with the achievement of 1.0 V OCV at 650°C [31]. Numerous significant progresses across the globe are discussed in various articles [3, 32–46].

The fabrication strategies were extended from binary to ternary oxide electrolytes. The fabrication of multiple oxide electrolytes faced difficulties with single-phase formation because of the presence of several oxides and their different crystallization kinetics. The possibility of developing a single-phase ternary oxide thin film was advanced with the successful fabrication of lead zirconate titanate (PZT) film via metallo-organic decomposition (MOD) and sol-gel route in the 1980s [18, 47, 48]. For the first time, phase-pure ternary oxide electrolyte film of Yb-doped strontium zirconate (YDSZ) was successfully obtained via sol-gel method [49]. Our group from Nanyang Technological University, Singapore, has recently reported the fabrication of a dense and crack-free yttria-doped barium zirconate (BZY) thin film by modified CSD technique along with various sintering strategies [38, 40, 50–52] at remarkably low sintering temperature of 800–1000°C. The following sections will give the detail about the various solution preparation strategies and sintering methods.

2. CSD methods

CSD techniques are specially characterized by its mass transport process (**Figure 1**) which maintains liquid phase as the mass transport media for the transportation of precursors from the source to the substrate. The major advantages of CSD method are homogeneity of the product and lower processing temperature compared to the temperature for solid-state sintering [29]. Morphological control over the deposited film can be gained through varying composition, viscosity, pH, concentration of the solution, etc.

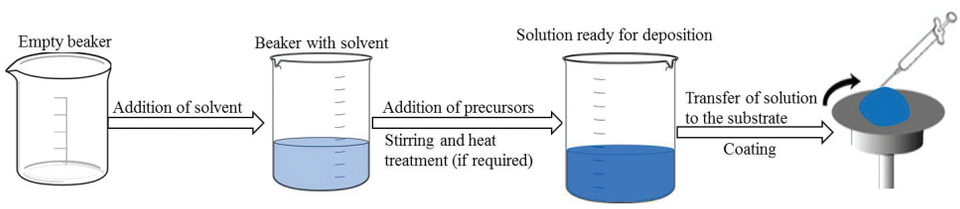

Figure 1. Chemical solution deposition technique.

Based on various requirements of different film morphology, CSD process can be categorized into three major groups: sol-gel process, chelate process, and MOD technique [53]. In this section, the CSD methodologies will be reviewed, with an emphasis on the underlying chemical aspects of the solution. The characteristics of the main three methods have been summarized in **Table 1**.

Method	Precursors and solvents	Control of chemistry	Simplicity
Sol-gel	• Metal alkoxides as precursors • Alcohols as solvents • Acid or base as catalyst • Water for polymerization	High	Low
Chelate	• Metal carboxylate, alkoxide, and β-diketonate as precursors • Acetylacetonate and acetic acid as chelating agent and solvents	Moderate	Moderate
Metallo-organic decomposition (MOD)	• Long-chain metal carboxylates such as 2-ethylhexanoate, dimethoxy dineodecanoate, and neodecanoate as precursors • Xylene as solvent (inert)	Low	High

Table 1. The comparison among three major CSD processes.

2.1. Sol-gel process

A classical sol-gel process typically involves metal alkoxides and alcohols ($M(OR)_x$ and ROH). Common alcohols are methanol and ethanol; 2-methoxyethanol and 1,3-propanediol are also widely used [54, 55]. The selection of cationic components and solvent is crucial for controlling subsequent hydrolysis and condensation reaction, which is the basis for the development of short polymeric species and metal-oxygen-metal (M–O–M) bond upon heat treatment. The reactions are described below [56]:

Hydrolysis:

$$M(OR)_x + H_2O \rightarrow M(OR)_{x-1}(OH) + ROH \tag{1}$$

Condensation (alcohol elimination):

$$2M(OR)_{x-1}(OH) + M_2O(OR)_{2x-3}(OH) + ROH \tag{2}$$

Condensation (water elimination):

$$2M(OR)_{x-1}(OH) + M_2O(OR)_{2x-2} + H_2O \tag{3}$$

The primarily evolution of inorganic networks occurs through the generation of small particle resulting into colloidal suspension (sol), followed by the formation of continuous network in liquid matrix (gel) [57, 58]. The formation of sol and gel is aided by addition of water, base, and acid [59]. Base and acid act as catalysts. Upon drying and heating, the gel gets converted into amorphous film along with densification. With further heating, amorphous film ceramizes and rate of densification slows down.

In case of multicomponent system, all the alkoxide precursors may not have equal tendency to get dissolved in the same solvent because of their different polarity and ionicity/covalency. Those alkoxides are sometimes pre-hydrolyzed so that the final solution becomes compositionally homogeneous.

Hydrolysis of a particular M–O–R bond depends on its polarity. As the bond polarity increases, the tendency of being hydrolysis also increases. This character plays an important role in determining the processing window which gives an amount of the ratio of reagent to water and precursor concentration. Addition of water to the solution should be controlled to hinder precipitation. Otherwise, powder formation will take place. There are two major strategies to address the problem of hydrolysis associated with polar compounds: alcohol exchange reaction and chelation. In both processes, susceptibility of the reactants toward water is reduced. The alcohol exchange reaction is described below [59]:

$$M(OR)_x + xR'OH \rightarrow M(OR')_x + xROH \tag{4}$$

or

$$M(OR)_x + xR'OH \rightarrow M(OR)_{x-1}(OR') + ROH + (x-1)R'OH \tag{5}$$

The alcohol, 2-methoxyethnol, is widely used for alcohol exchange reaction due to its bidentate nature. Hence, the newly generated alkoxide is less prone to hydrolysis, thereby allowing easy formation of gel instead of precipitate [35]. As for example, 2-methoxyethanol was used to dissolve Ba metal and partially substitute propoxide of zirconium propoxide for the fabrication of epitaxial BZY film. Acetic acid is used for chelation. In some typical film fabrication method, both the acetic acid and 2-methoxyethanol are used together [60]. As 2-methoxyethnol does not change the solution pH, it is often used for the dilution of solution.

2.2. Chelate process

This is a specialized process of sol-gel technique which employs chelation reaction as the key process in the preparation of the precursor solution. This process with a wide range of application and variety of chemical compositions has opened a separate branch called chelate process. The process aims at the reduction in over-reactive tendency of alkoxides via addition of acetylacetonate or diethanolamine. In most compositions, metal carboxylate, β-diketonate, and alkoxides are used as precursors [59]. Mostly, transition metal alkoxides show polarity with high tendency toward rapid hydrolysis and condensation, requiring complexing or chelating ligands to limit uncontrolled reactions. Acetic acid and acetylacetone are added to the precursor solution to alleviate the issue. Acetic acid can act as both chelating and bridging agent, while acetylacetone only acts as chelating agent. This chelating agent blocks hydrolysis site with the replacement of reactive alkoxide ligand. A typical reaction with acetic acid is described below:

$$M(OR)_n + xCH_3COOH \rightarrow M(OR)_{n-x}(CH_3COO)_x + xROH \tag{6}$$

This typical reaction states that the species contains both the acetate and alkoxide ligands. Being bidentate in nature [61] and sterically larger than alkoxy group, the acetate ligands are not much susceptible to hydrolysis. In addition to this, acetylacetone plays the role of stabilizer of colloidal solution as well since it prevents aggregation of colloidal particles by creating steric hindrance [62]. In a typical chelate process, YDSZ was prepared via chelate route using acetylacetone [49]. This chelate process has been widely used to fabricate YSZ and BZY films for SOFC electrolytes [36, 40, 50–52, 63].

2.3. Metallo-organic decomposition (MOD)

This method involves high molecular weight precursors such as water-insensitive carboxylates and 2-ethylhexanoates. This process is less common than the other methods [59, 64]. This method is straightforward without necessitating precise control of the chemistry. Long-chain carboxylate compounds such as lead 2-ethylhexanoate, titanium dimethoxy dineodecanoate, zirconium neodecanoate, etc. are used as precursors, whereas the common solvent is xylene. The method involves simply dissolution of the metallo-organic compounds in a common solvent. The organic moieties of long-chain length compounds enhance dissolution tendency and concomitantly hinder hydrolysis tendency. They are normally dissolved in common solvent such as xylene [59, 64–66]. As these precursors are water insensitive and nonreactive to one another, they do not undergo any structural or chemical change [56]. This process is the simplest one among the three methods since no skill for controlling the hydrolysis and condensation is necessary. Still, this process suffers from several limitations. First, the large organic chains may cause crack during its decomposition upon heat treatment. Second, modification of the solution properties is limited; hence, the microstructure of the thin film cannot be tailored. This method has been applied specially for the ferroelectric materials [56]. The application of this method is not so popular in the field of SOFCs.

2.4. Other processing routes

Although the abovementioned three processes have found extensive application, there are several other routes such as Pechini method (old method), aqueous solution, citrate, nitrate routes, etc. [56, 59]. Pechini method is an aqueous chemical route which involves dissolution of metal cations and hydroxycarboxylic acid (such as citric acid, etc.) and ethylene glycol in deionized water. Till date, simple Pechini method has not shown any remarkable progress in the field of SOFC electrolytes. Pechini method modified with ethylenediaminetetraacetic acid (EDTA) has been proved to be an efficient technique for the fabrication of nonporous thin-film gadolinia-doped barium cerate (BCG) for SOFC [67]. Citrate process is also similar to the Pechini method [56] without involving ethylene glycol. This method modified with EDTA as chelating agent successfully produced electrolyte film without through-film crack [38]. Aqueous method includes dissolution of metal nitrates or chlorides and other polymerizing agents such as polyvinylpyrrolidone (PVP) in deionized water [34]. A SOFC cell with 0.5 μm thick crack-free YSZ electrolyte film was fabricated via this method. YSZ thin films obtained by both the aqueous and the nonaqueous processes are identical as per the surface morphology, which gives the direction toward the development of aqueous method in future.

2.5. Combined colloidal CSD method

The limitation of sol-gel, chelate, and MOD processes lies in obtaining film thicker than 0.5 μm with the application of single-layer coating [68]. Therefore, the multi-coating approach was required to obtain thicker film. Still, there is limitation for obtaining crack-free film thicker than 10 μm due to the constraining effect of the substrate. Hence, combined colloidal CSD method was introduced [32, 63, 68, 69]. This method involves addition of pre-synthesized nano-powder to CSD solution. This newly formed system consists of precursors, nano-powder (either synthesized via sol-gel route or commercially purchased), and at least one solvent [69]. Nanoparticles are introduced in the chemical solution to encounter the external constraint due to the presence of substrate and reduce the extent of differential densification in the planar dimension. As the metal-oxide network shrinks faster than the substrate, shrinkage mismatch occurs between the film and the substrate. Since the nanoparticles are supposed to sinter at a significantly lower rate than the metal-oxide framework [31], nanoparticles were added to the solution. To date, there are several significant research works on the YSZ thin film and doped ceria with the thickness ranging from nanometer to several micrometer via CSD method or combined CSD method [32–34, 39, 60, 63, 68, 70–72]. Several groups have already made micro-SOFCs based on CSD techniques [39, 70, 72].

3. Deposition techniques

The precursor solution is deposited over the substrate via a number of coating techniques. The most widely used coating techniques are spin coating, dip coating, and spray coating, as illustrated in **Figure 2**. In this section, the film deposition techniques and their application to SOFC electrolytes will be discussed.

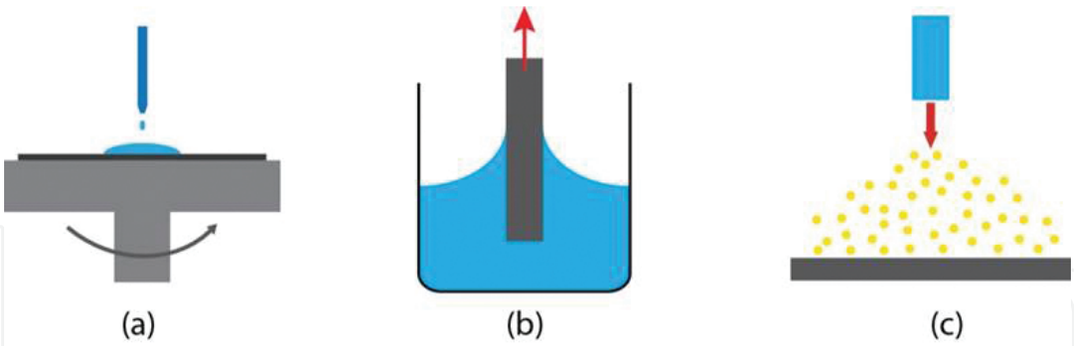

Figure 2. Schematic diagrams of (a) spin, (b) dip, and (c) spray coating.

3.1. Spin coating

Spin coating is a simple process to deposit uniform thin films on relatively flat substrates (**Table 2**). Typically, the substrate to be coated is held in place by vacuum chuck, and the coating solution is dispensed onto the substrate. The substrate is then accelerated to the desired rotation speed for certain duration to obtain desirable film thickness. The excess liquid is spread out from the substrate due to the action of centrifugal force, leaving a thin uniform coating on the surface of the substrate. The major advantages of spin coating are reproducibility, uniformity, simplicity, ability to use different substrate materials, and low cost. The main disadvantage of the method is the requirement of the smooth and flat substrate.

Technique	Description	Advantages	Disadvantages	Application
Spin coating	Evenly coats the substrates with CSD solution due to the rotation of the substrate placed on vacuum chuck	• Simplicity • Thin and uniform coating • Low cost	• Relatively low throughput • Requirement of smooth and flat substrate	• Semiconductors • Photoresist • Insulators • Organic semiconductors • SOFC electrolyte and cathode, etc.
Dip coating	Immersion of a substrate into CSD solution and its subsequent removal	• Simplicity • Controllable film thickness • Coating on irregular and complex shaped substrates	• Variation in film thickness • Coating on the both sides of the substrate simultaneously	• Flat or cylindrical substrates • Optical coating on glass, etc.
Spray coating	Deposition of the aerosol of CSD solution, via a nebulizer or a nozzle, on the substrate	• Uniform coating even on highly structured surfaces	• Expensive	• Coating on dielectrics • Coating for corrosion protection, etc.

Table 2. Three coating techniques used for CSD processes.

The thickness of the coating film is influenced by the spinning speed and time as well as the solution viscosity. According to the empirical equation, the film thickness (t) is inversely proportional to the square root of the spin speed (ω: angular velocity) [73]:

$$t \propto \frac{1}{\sqrt{\omega}} \tag{7}$$

Spinning speed of 2000–3000 rpm is usually used for depositing SOFC electrolyte thin films. The film thickness of 30–100 nm is obtained after one layer deposition depending on the viscosity of the solution and duration of spinning. Typical film thicknesses of SOFC electrolytes are kept usually below 1 μm [31, 34, 38, 44, 74–76]. Several works on electrolyte fabrication with spin coating technique have been reported in the field of SOFCs [31, 38, 76].

3.2. Dip coating

Dip coating is a simple, flexible, and cost-effective solution deposition technique that allows coating on both large area and complex shaped substrates. The process involves immersion of substrate in the solution and subsequent removal. A coherent liquid film is entrained on the withdrawal of the substrate from the coating fluid, and the film is subsequently consolidated by drying and accompanying chemical reactions. Typical film thickness obtained is in the micrometer range.

The process of film formation follows fluid mechanical equilibrium between the entrained film and the receding liquid. The equilibrium is governed by several forces. Viscous drag and gravitational forces play the most significant role. Other forces like surface tension, inertial force, or disjoining pressure also play an important role [77]. A competition between these forces in the film deposition region governs the thickness of the film. The film thickness is given by the Landau-Levich equation [78, 79]:

$$t = 0.94 \frac{\eta U^{2/3}}{\gamma^{1/6} \rho g^{1/2}} \tag{8}$$

where η is the liquid viscosity, U is the withdrawal speed, γ is the surface tension, and ρ is the liquid density. This technique is not applied for electrolyte fabrication of SOFCs because this technique aids in the formation of film on both sides of the substrate.

3.3. Spray coating

The spray coating technique is based on the transformation of a liquid precursor solution into a fine aerosol by atomizer or nebulizer [80]. These fine droplets are then deposited on a substrate surface either with carrier gas or with an electrostatic field or by gravity. The substrate may be at room temperature or above. The different spray techniques are mainly distinguished by the method of atomization [81] and, hence, produce different morphologies of the film. For

example, YSZ thin films deposited using electrostatic spray deposition (ESD) and pressurized spray deposition (PSD) on the substrate [82] showed different morphologies from dense to porous. Other parameters such as flow rate, substrate temperature, and deposition time also influence the morphology of the deposited film. The flow rate should not exceed a certain value for a particular composition of the solution and associated parameters; otherwise, cracks may form. Spray pyrolysis has also been applied for the deposition of SOFC electrolyte thin films [71, 83, 84]. To mention a significant work, a gastight bilayer electrolyte fabricated via spray coating technique demonstrated a power density of 750 mW/cm^2 with the achievement of 1.01 V OCV at 770°C [84].

4. Solution chemistry

The chemistry of the solution determines the morphology of the film. A wide knowledge of chemistry is required to formulate workable solution. Attention must be paid to several issues such as reactivity among the precursors and solvent, homogeneity of the solution, solvent vapor pressure, wettability of the solvent to the substrate surface, reaction products, pH and viscosity of the solution, etc.

The hydrolysis and condensation reaction needs to be controlled carefully to tailor the morphology of the film. Precursors with more than two hydrolysis sites are highly sensitive toward hydrolysis and form three-dimensional networks during gelation, which provides rigidity to the M–O–M network and inhibits densification of the final sintered film. Water, chelating agent, and modifying ligand are added to block the hydrolysis sites of the precursors. Precursors with two unblocked sites form linear structure, which facilitates almost stress-free densification in all directions.

Transition metal alkoxide precursors require special attention because of their high reactivity and inclination toward coordination expansion. Due to their coordination expansion, these metals become coordinatively unsaturated. In order to satisfy their coordination, they sometimes get integrated with water and subsequently undergo precipitation. These highly sensitive alkoxides need to be handled in glove box initially. Diethanolamine (DEA) and triethanolamine (TEA) are generally used to stabilize alkoxides of transition metals [85]. Stabilization also occurs via chelation and alcohol exchange method. After modification, they do not react with moisture in air.

Compositional homogeneity is desirable for the successful fabrication of film without any defect. Striation is a very common problem associated with heterogeneous solution. Striation is a series of ridges resulting into variation in thickness throughout the film [86]. Heterogeneity is associated with the separation of polymer-rich and polymer-deficient portion of the solution due to the presence of both polar and nonpolar precursors in a multicomponent system. Therefore, a single solvent with both the characters is desirable to maintain homogeneity. For example, 2-methoxyethanol having both the characters is a widely used solvent. Heterogeneous solution also results from the mixture of the solvents of different characters such as specific gravity. Phase separation is another issue associated with the heterogeneous solution, which

occurs due to the different rate of the hydrolysis of different components. Refluxing treatment is carried out to address the issue. This treatment helps in random combination of cations [87].

Solvent vapor pressure is one important parameter because solvent determines the film thickness and its rigidity. The short-chain alcohols are generally used for thinner film, while the long-chain alcohols are for thicker films [88, 89]. Short-chain alcohols have higher tendency to leave film faster because of its higher vapor pressure. Higher vapor pressure generates higher capillary force, which drives precursors in greater proximity, thereby causing higher cross-linking among metal-oxide precursors. This cross-link offers rigidity to the film, producing crack in the film [29]. On the other hand, the solvents with low vapor pressure hinder cross-linking reaction, resulting into the crack-free film.

The solution pH and the product generated during condensation reaction have immense influence over the rate of condensation reaction [90, 91]. The reaction products are alcohol and water. Alcohol is eliminated during deposition, which forces the condensation reaction to shift toward the forward direction. Thus, more M–O–M cross-linked network forms. The presence of water in the solution or in the ambient atmosphere slows down the condensation process. The early work showed that the density of the film was enhanced with the presence of more water [91].

Viscosity and concentration of the solution are other variables to control the thickness and the initiation of the crack throughout the film. Early work demonstrated that the higher concentration of the solution produced the thicker film with crack. As per the literature report, the critical thickness limit for the film is governed by the following equation [92]:

$$h = \frac{K_{IC}}{\sigma \Omega_C(\Sigma)} \tag{9}$$

where h is the critical thickness, K_{IC} is the critical stress intensity factor, σ is the tensile stress in the film, and $\Omega_c(\Sigma)$ is the ratio of Young's modulus of the film to that of the substrate.

Solution properties	Effects
Polar and nonpolar character of the solvent	Striation: variation of film thickness
Vapor pressure of solvent	Cracking, dewetting
Concentration and viscosity	Film thickness, crack formation, and uniformity of film
Modifying ligand	Possible formation of 2D network instead of 3D network
Long-chain polymer	Low tensile stress in the film
Presence of water	Slower condensation reaction
Presence of alcohol	Faster condensation reaction

Table 3. Solution properties.

The equation describes the dependence of the critical thickness on the tensile stress exerted on it. Critical thickness decreases with the increase in tensile stress. The critical thickness of film can be increased with the use of longer-chain solvents [89]. Another approach to deal with this issue is to increase the adhesion between the substrate and film [29]. During shrinkage, formation of crack occurs due to the large mismatch of thermal expansion coefficients of the film and the substrate. The strain energy is relieved via the formation of crack, but this strain energy can be balanced by the strength of adhesion of the film to the substrate. Excellent substrate-film adhesion may provide relaxation for the fabrication of thicker film. Therefore, modification of substrate surface before deposition has significance. The properties of solution and their effects are summarized in **Table 3**.

5. Heat treatment

5.1. Physical changes occurring during heat treatment

Several phenomena occur after deposition of film. They are hydrolysis, drying, condensation, gelation, and densification [93]. Generally, gelation and drying phenomena occur simultaneously during deposition and continue afterward. The deposited film acts as a viscoelastic solid, which is an inorganic framework with organic moieties entrapping solvent [94]. These organics are removed with heat treatment via either pyrolysis or thermolysis process. Pyrolysis occurs in the presence of oxygen, whereas thermolysis occurs in the absence of oxygen. Followed by organic removal, crystallization occurs. Partial densification takes place in the amorphous stage, while the final densification occurs after crystallization.

Hydrolysis-condensation reaction generally occurs in the temperature range of 80 to 400°C. This reaction generates water and alcohols, which are removed via drying process. During drying or organic removal process, a gas-liquid interface is generated within the pores because of the evaporation of liquid. In addition to this, gas-solid and solid-liquid interfaces also exist. These interfaces generate pressure, which gives birth to capillary contraction. The magnitude of capillary contraction depends on the specific energies across these interfaces, nature of the liquid, and pore size. This capillary contraction is responsible for producing the driving force to the collapse of the amorphous network. This driving force is proportional to the pore diameter. At this stage, the film might be prone to crack because of the pressure differential occurring due to the presence of pores with different diameters. The total stress due to drying, capillary contraction, and network consolidation is normally around 100 MPa [95].

Gelation occurs due to the continuous removal of water and organics. During gelation, M–O–M network starts forming. With the heat treatment, a good number of M–O–M linkages form and densification proceeds. Skeletal densification occurs with the structural rearrangement of M–O–M bond. The structure approaches to the state of metastable liquid in the temperature range of 400–600°C. With the increase in temperature, viscous flow occurs [51], followed by crystallization above 600°C. However, crystallization starts after complete removal of organics. Crystallization kinetics depends on its own nature of crystallization (i.e., glass formers have slow rate of crystallization, while other oxides show

moderate to high rate of crystallization) and the heating schedule. Structural relaxation occurs during crystallization process. The presence of organic groups delays structural relaxation and crystallization to a higher temperature. Following this principle, crystallization is purposefully delayed so that densification gets over before crystallization [50]. All the processes overlap one another. There is no distinct temperature range. Depending on the solution chemistry, the processes may occur faster or slower.

5.2. Phase transformation

After completion of pyrolysis, liquid film transforms to the metastable amorphous stage. With further heat treatment to the higher temperature, the amorphous film transforms to the crystalline stage via nucleation and growth process. Thermodynamic driving force plays a role behind this transformation. This force comes from the difference between the free energies of those two states. **Figure 3** describes the phenomena. The driving force for transformation to the final stage depends on the crystallization temperature and the free energy associated with both stages of the films.

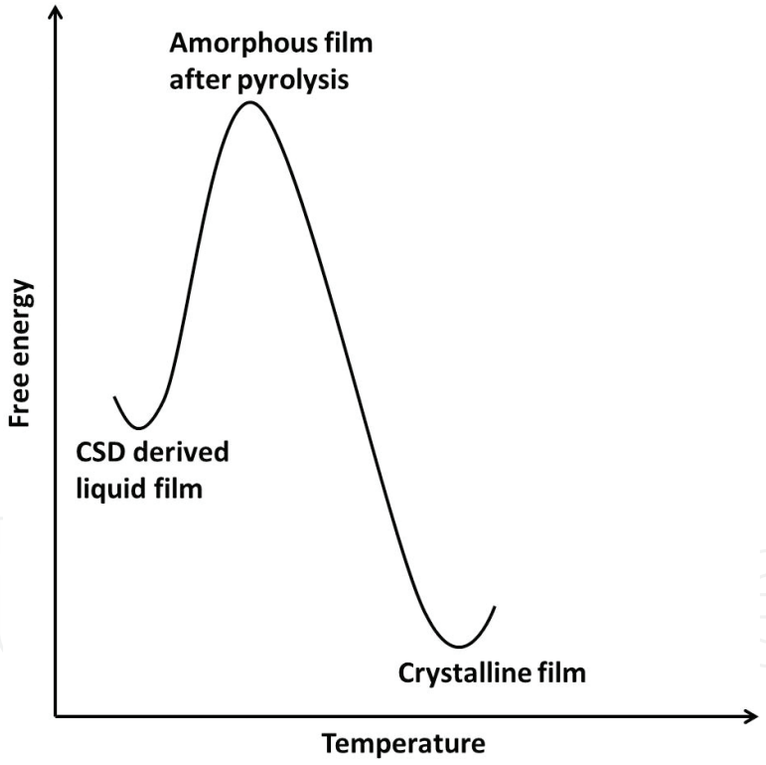

Figure 3. Thermodynamic driving force associated with phase transformation.

Crystallization kinetics starts with the nucleation, which is quite similar to the transformation from amorphous glassy to crystalline phase. The different features of CSD-derived film are associated with the presence of residual hydroxyl group, excess surface area associated with the porosity, and skeletal density. However, the nucleation and growth theory applicable for glass-ceramic science also applies to the transformation of the CSD-derived film [96]. Gibb's

free energy (ΔG) associated with the driving force for crystallization is expressed by the following equation:

$$\Delta G = -\frac{4}{3}\pi r^3(\Delta G_v) + 4\pi r^2\sigma \tag{10}$$

where ΔG_v and σ are Gibb's free energies associated with unit volume and surface, respectively, and r is the radius of the nucleus formed during nucleation. The equation gives rise to the concept of critical radius. A critical radius (r^*) is the minimum required radius for the formation of stable nucleus. The derivative of the above equation with respect to radius gives the relationship between the critical radius (r^*) and the energy barrier (ΔG^*) required to be overcome to form a stable nucleus, which is described by the following equation:

$$\Delta G^{\star} = \frac{16\pi\sigma^3}{3(\Delta G_v)^2} \tag{11}$$

This equation holds good for homogeneous nucleation where the amorphous film does not encounter any nucleation site. Heterogeneous nucleation occurs when the amorphous material can rest on nucleation site, i.e., any surface such as impurity, substrate, grain boundaries, etc. In case of heterogeneous nucleation, the above equation is modified by the contact angle term, $f(\theta)$, associated with the substrate surface (roughness) and the crystal:

$$\Delta G^*_{hetero} = \frac{16\pi\sigma^3}{3(\Delta G_v)^2} f(\theta) \tag{12}$$

where

$$f(\theta) = \frac{2 - 3cos\theta + cos^3\theta}{4} \tag{13}$$

where θ is the contact angle between the substrate surface and the crystal. Heterogeneous nucleation is always energetically favorable because of the lower energy barrier due to the presence of the preferential nucleation sites.

Rates of nucleation and growth with respect to the temperature coordinate are important factors for tailoring microstructure of the film. Higher nucleation rate gives finer microstructure, while

higher rate of growth with lower nucleation gives coarse microstructure. The relationship among temperature, nucleation density (number of nuclei in a cubic meter volume), and free energy barrier is governed by the following equation:

$$n^* \infty \exp\left(-\Delta \frac{G^*}{RT}\right) \tag{14}$$

As the temperature is raised, higher energy is provided to overcome the nucleation barrier. Therefore, the rate of nucleation increases. After nucleation rate reaches the maximum height, it declines with further increase of temperature. Driving force for crystallization gets reduced as the material approaches its melting temperature [94] and barrier height to nucleation increases. This type of phenomena gives rise to a bell-shaped curve. The same kind of curve is also applicable for the growth rate. A typical curve is presented in **Figure 4**.

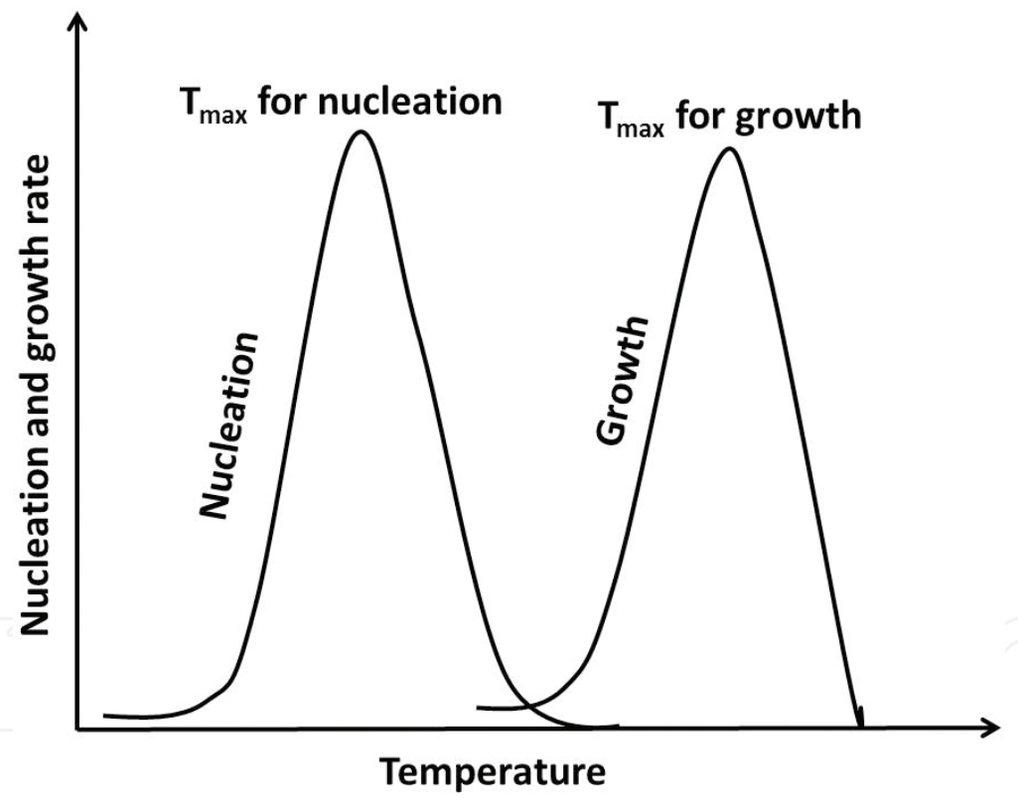

Figure 4. Schematic of nucleation and growth locus in temperature coordinate for homogeneous nucleation (ideal case).

The nucleation curve is followed by the growth rate curve on the temperature coordinate, and they overlap to some extent. The area of the overlapped region depends on chemical composition of the solution, fabrication procedure, and prior heat treatment history. The representation in **Figure 4** is applicable for the homogeneous nucleation [97] as the apex of the growth rate curve lies at higher temperature than that of the nucleation rate curve. Based

on the calculation, the maximum nucleation rate may be located at higher temperature than the maximum growth rate in case of heterogeneous nucleation. The schematic representation of these phenomena is depicted in **Figure 5**.

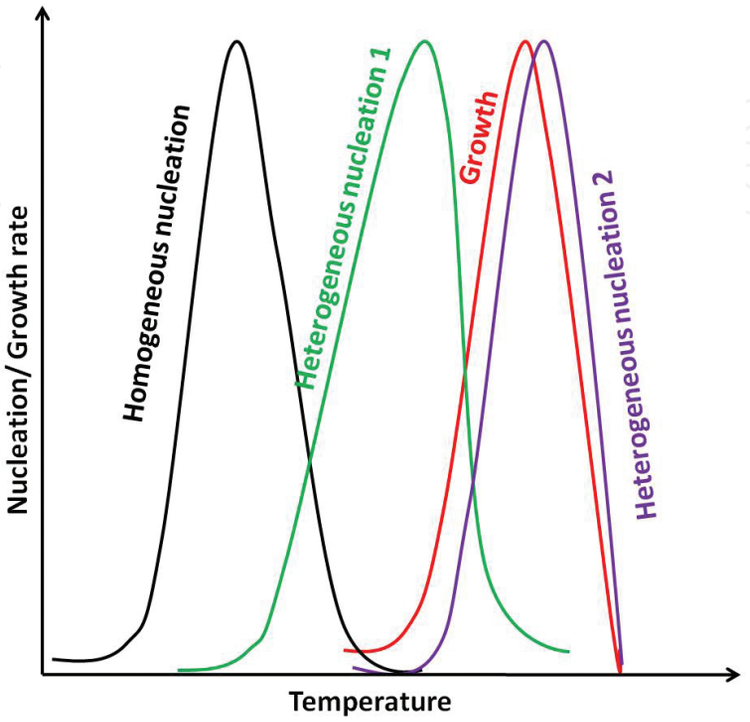

Figure 5. Schematic of nucleation and growth locus in temperature coordinate for heterogeneous nucleation and homogeneous nucleation with low interfacial energy.

In case of the film on the substrate, crystallization is affected due to the presence of two separate nucleation events. One is the surface nucleation of the film which is homogeneous in nature, and the other one is the interfacial nucleation on the substrate. Nucleation occurs on both the substrate and film surfaces, as represented in **Figure 6**.

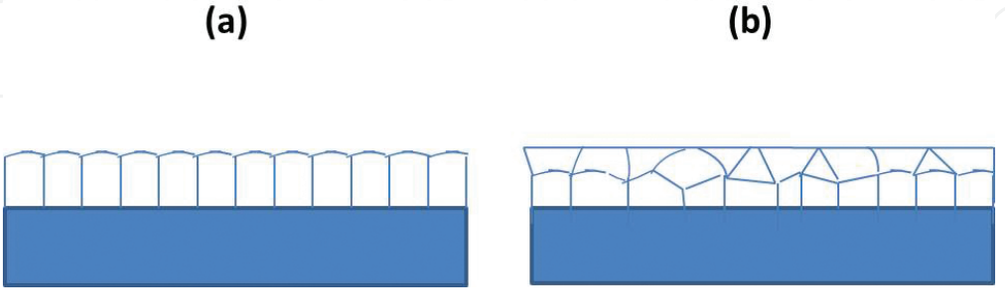

Figure 6. Kinetic competition between two nucleation events on the interface and on the surface of the film: (a) nucleation at the interface only and (b) nucleation at both interface and surface of the film.

Heterogeneous nucleation occurs at the substrate first, while homogeneous nucleation and growth event occur on the surface of the film; growth direction is opposite to each other. The

density of nucleus is higher at the interface than at the surface of the film. The dominance of one process over the other depends on the crystallization temperature of the film. The film with lower crystallization temperature shows smaller difference in the kinetics of two nucleation events, than the film with higher crystallization temperature [98].

5.3. Salient features

Heating rate also has impact over the kinetics of these processes. Various heating schedules with several heating rates are used to keep control over the microstructure of the film. Keddie and Giannelis experimented on the effect of heating rate (0.2–8000°C/min) for the densification of TiO_2 film as model system [99] and found that the thinnest film was obtained with the highest heating rate. Rapid thermal annealing (RTA) and isothermal heat treatment at high temperature are two useful processes for thin-film fabrication [50, 99].

Effect of the substrate is another important issue for the orientation of thin film. A highly oriented phase-pure barium zirconate ($BaZrO_3$) film fabricated via sol-gel route was epitaxially grown on (100) plane on strontium titanate ($SrTiO_3$) at 800°C, while the same solution deposited on $LaAlO_3$ substrate had produced film with random structure [35].

6. Conclusion

The CSD method combined with right sintering strategy is the blessing in the sector in SOFC manufacturing. The growth of the SOFC technologies is restricted mostly to the R&D sector because suitable position in the market of clean energy sources is yet to be achieved. The hurdle behind commercialization of intermediate to low-temperature SOFCs arises from its high manufacturing cost. The CSD method has proved to be a potential technique in this field. Although this method did not find application for over a century after its discovery, now it is progressing exponentially with time in all the sectors of thin film. The fabrication of crystalline YSZ and YDSZ film has initiated a new era in the manufacturing of SOFCs, which ensures the rapid commercialization of SOFCs in the near future. This technology requires low investment cost while demanding a good command over chemistry. Therefore, CSD technology is facing several difficulties related to the fabrication strategies. The major issues are preparation of homogeneous solution for multicomponent system, preservation of the solution for a considerable duration without aging, handling with highly reactive precursors, controlling the hydrolysis-condensation reaction, gelation kinetics, solvent evaporation, choice of environment-friendly chemicals without compromising necessary properties, selection of appropriate deposition technique, right heating schedule and environment, determination of critical thickness limit, etc. Many challenges have been successfully dealt with, while a good number of issues need more attention. However, recent success stories predict the bright future of this technology. Presently, effort is also given to the water-based CSD method.

Author details

Mridula Biswas and Pei-Chen Su*

*Address all correspondence to: peichensu@ntu.edu.sg

School of Mechanical and Aerospace Engineering, Nanyang Technological University, Singapore, Singapore

References

[1] Hong S, Bae J, Koo B, Kim YB. High-performance ultra-thin film solid oxide fuel cell using anodized-aluminum-oxide supporting structure. Electrochemistry Communications. 2014;47:1–4.

[2] Su PC, Chao CC, Shim JH, Fasching R, Prinz FB. Solid oxide fuel cell with corrugated thin film electrolyte. Nano Letters. 2008;8(8):2289–2292.

[3] Shim JH, Chao CC, Huang H, Prinz FB. Atomic layer deposition of yttria-stabilized zirconia for solid oxide fuel cells. Chemistry of Materials. 2007;19(15):3850–3854.

[4] Huang H, Nakamura M, Su P, Fasching R, Saito Y, Prinz FB. High-performance ultrathin solid oxide fuel cells for low-temperature operation. Journal of The Electrochemical Society. 2007;154(1):B20–B24.

[5] Huang H, Gür TM, Saito Y, Prinz F. High ionic conductivity in ultrathin nanocrystalline gadolinia-doped ceria films. Applied Physics Letters. 2006;89(14):3107.

[6] Su PC, Prinz FB. Nanoscale membrane electrolyte array for solid oxide fuel cells. Electrochemistry Communications. 2012;16(1):77–79.

[7] Chao CC, Hsu CM, Cui Y, Prinz FB. Improved solid oxide fuel cell performance with nanostructured electrolytes. ACS Nano. 2011;5(7):5692–5696.

[8] Choi H, Cho GY, Cha SW. Fabrication and characterization of anode supported YSZ/GDC bilayer electrolyte SOFC using dry press process. International Journal of Precision Engineering and Manufacturing-Green Technology. 2014;1(2):95–99.

[9] Greene J, Wickersham C, Zilko J, Welsh L, Szofran F. Morphological and electrical properties of rf sputtered Y_2O_3-doped ZrO_2 thin films. Journal of Vacuum Science & Technology. 1976;13(1):72–75.

[10] Croset M, Schnell JP, Velasco G, Siejka J. Composition, structure, and ac conductivity of rf-sputtered calcia-stabilized zirconia thin films. Journal of Applied Physics. 1977;48(2):775–780.

[11] Isenberg A. Energy conversion via solid oxide electrolyte electrochemical cells at high temperatures. Solid State Ionics. 1981;3:431–437.

[12] Nakagawa N, Kuroda C, Ishida M. Preparation of thin-film zirconia electrolyte fuel-cell by rf-sputtering. Denki Kagaku. 1989;57(3):215–218.

[13] Negishi A, Nozaki K, Ozawa T. Thin-film technology for solid electrolyte fuel cells by the rf sputtering technique. Solid State Ionics. 1981;3:443–446.

[14] Srivastava P, Quach T, Duan Y, Donelson R, Jiang S, Ciacchi F, et al. Electrode supported solid oxide fuel cells: Electrolyte films prepared by dc magnetron sputtering. Solid State Ionics. 1997;99(3):311–319.

[15] Uhlenbruck S, Nédélec R, Sebold D, Buchkremer HP, Stöver D. Electrode and electrolyte layers for solid oxide fuel cells applied by physical vapor deposition (PVD). ECS Transactions. 2011;35(1):2275–2282.

[16] Maskalick N, Sun C. Sintered zirconia electrolyte films in high-temperature fuel cells. Journal of The Electrochemical Society. 1971;118(8):1386–1391.

[17] Ganguli D, Kundu D. Preparation of amorphous ZrO_2 coatings from metal-organic solutions. Journal of Materials Science Letters. 1984;3(6):503–504.

[18] Fukushima J, Kodaira K, Matsushita T. Preparation of ferroelectric PZT films by thermal decomposition of organometallic compounds. Journal of Materials Science. 1984;19(2): 595–598.

[19] Schwartz RW, Schneller T, Waser R. Chemical solution deposition of electronic oxide films. Comptes Rendus Chimie. 2004;7(5):433–461.

[20] Jagannathan K, Tiku S, Ray H, Ghosh A, Subbarao EC. Solid electrolytes and their applications. In: Technological Applications of Solid Electrolytes. Springer; US. 1980. pp. 201–259.

[21] Chiodelli G, Magistris A, Scagliotti M, Parmigiani F. Electrical properties of plasma-sprayed yttria-stabilized zirconia films. Journal of Materials Science. 1988; 23(4):1159–1163.

[22] Setoguchi T, Sawano M, Eguchi K, Arai H. Application of the stabilized zirconia thin film prepared by spray pyrolysis method to SOFC. Solid State Ionics. 1990;40:502–505.

[23] de Souza S, Visco SJ, De Jonghe LC. Reduced-temperature solid oxide fuel cell based on YSZ thin-film electrolyte. Journal of The Electrochemical Society. 1997; 144(3):L35–L37.

[24] Charpentier P, Fragnaud P, Schleich D, Gehain E. Preparation of thin film SOFCs working at reduced temperature. Solid State Ionics. 2000;135(1):373–380.

[25] Ebelmen J. Sur les éthers siliciques. Comptes Rendus de l'Académie des Sciences. 1844;19:398–400.

[26] Dislich H. Sol-gel: Science, processes and products. Journal of Non-Crystalline Solids. 1986;80(1):115–121.

[27] Schroeder H. Properties and applications of oxide layers deposited on glass from organic solutions. Optica Acta. 1962;9:249.

[28] Dislich H, Hussmann E. Amorphous and crystalline dip coatings obtained from organometallic solutions: Procedures, chemical processes and products. Thin Solid Films. 1981;77(1):129–140.

[29] Kueper TW, Visco SJ, De Jonghe L. Thin-film ceramic electrolytes deposited on porous and non-porous substrates by sol-gel techniques. Solid State Ionics. 1992;52(1):251–259.

[30] Mehta K, Xu R, Virkar AV. Two-layer fuel cell electrolyte structure by sol-gel processing. Journal of Sol-Gel Science and Technology. 1998;11(2):203–207.

[31] Oh EO, Whang CM, Lee YR, Park SY, Prasad DH, Yoon KJ, et al. Extremely thin bilayer electrolyte for solid oxide fuel cells (SOFCs) fabricated by chemical solution deposition (CSD). Advanced Materials. 2012;24(25):3373–3377.

[32] Courtin E, Boy P, Piquero T, Vulliet J, Poirot N, Laberty-Robert C. A composite sol-gel process to prepare a YSZ electrolyte for solid oxide fuel cells. Journal of Power Sources. 2012;206:77–83.

[33] Bailly N, Georges S, Djurado E. Elaboration and electrical characterization of electro-sprayed YSZ thin films for intermediate temperature-solid oxide fuel cells (IT-SOFC). Solid State Ionics. 2012;222:1–7.

[34] Chen YY, Wei WCJ. Processing and characterization of ultra-thin yttria-stabilized zirconia (YSZ) electrolytic films for SOFC. Solid State Ionics. 2006;177(3):351–357.

[35] Paranthaman M, Shoup SS, Beach DB, Williams RK, Specht ED. Epitaxial growth of $BaZrO_3$ films on single crystal oxide substrates using sol-gel alkoxide precursors. Materials Research Bulletin. 1997;32(12):1697–1704.

[36] Schneller T, Schober T. Chemical solution deposition prepared dense proton conducting Y-doped $BaZrO_3$ thin films for sofc and sensor devices. Solid State Ionics. 2003;164(3):131–136.

[37] Groß B, Engeldinger J, Grambole D, Herrmann F, Hempelmann R. Dissociative water vapour absorption in $BaZr_{0.85}Y_{0.15}O_{2.925}/H_2O$: Pressure-compositions isotherms in terms of fermi-dirac statistics. Physical Chemistry Chemical Physics. 2000;2(2):297–301.

[38] Xie H, Su PC. Fabrication of yttrium-doped barium zirconate thin films with sub-micrometer thickness by a sol-gel spin coating method. Thin Solid Films. 2015; 584:116–119.

[39] Rupp JL, Infortuna A, Gauckler LJ. Thermodynamic stability of gadolinia-doped ceria thin film electrolytes for micro-solid oxide fuel cells. Journal of the American Ceramic Society. 2007;90(6):1792–1797.

[40] Biswas M, Xie H, Su PC. Low temperature synthesis of sub-micrometer yttria-doped barium zirconate thin films by modified chemical solution deposition technique. ECS Transactions. 2015;68(1):481–488.

[41] Matsuzaki Y, Hishinuma M, Yasuda I. Growth of yttria stabilized zirconia thin films by metallo-organic, ultrasonic spray pyrolysis. Thin Solid Films. 1999;340(1):72–76.

[42] Butz B, Störmer H, Gerthsen D, Bockmeyer M, Krüger R, Ivers-Tiffée E, et al. Microstructure of nanocrystalline yttria-doped zirconia thin films obtained by sol-gel processing. Journal of the American Ceramic Society. 2008;91(7):2281–2289.

[43] García-Sánchez M, Peña J, Ortiz A, Santana G, Fandiño J, Bizarro M, et al. Nanostructured ysz thin films for solid oxide fuel cells deposited by ultrasonic spray pyrolysis. Solid State Ionics. 2008;179(7):243–249.

[44] Abakevičienė B, Žalga A, Tautkus S, Pilipavičius J, Navickas E, Kareiva A, et al. Synthesis of YSZ thin films by the novel aqueous sol-gel citrate-precursor method. Solid State Ionics. 2012;225:73–76.

[45] Zhang L, Yang W. High-performance low-temperature solid oxide fuel cells using thin proton-conducting electrolyte with novel cathode. International Journal of Hydrogen Energy. 2012;37(10):8635–8640.

[46] Chung BW, Chervin CN, Haslam JJ, Pham AQ, Glass RS. Development and characterization of a high performance thin-film planar SOFC stack. Journal of the Electrochemical Society. 2005;152(2):A265–A269.

[47] Budd KD, Key S, Payne D, Steele BCH. Sol-gel processing of $PbTiO_3$, $PbZrO_3$, PZT and PLZT thin films. In: British Ceramics Proceedings. Institute of Ceramics; Stoke-on-Trent, England. 1985.

[48] Dey S, Budd KD, Payne DA. Thin-film ferroelectrics of PZT of sol-gel processing. IEEE Transactions on Ultrasonics, Ferroelectrics, and Frequency Control. 1987;35(1):80–81.

[49] Eschenbaum J, Rosenberger J, Hempelmann R, Nagengast D, Weidinger A. Thin films of proton conducting $SrZrO_3$-ceramics prepared by the sol-gel method. Solid State Ionics. 1995;77:222–225.

[50] Xie H, Biswas M, Fan L, Li Y, Su PC. Rapid thermal processing of chemical-solution-deposited yttrium-doped barium zirconate thin films. Submitted to Surface and Coating Technology. 2016.

[51] Biswas M, Xie H, Baek JD, Su PC. Fabrication of yttria-doped barium zirconate electrolyte with submicrometer thickness via low temperature viscous flow sintering. Submitted to Surface and Coating Technology. 2016.

[52] Biswas M, Xie H, Baek JD, Su PC. Low temperature sintering of gas-tight yttria-doped barium zirconate electrolyte with sub-micrometer thickness. submitted to Journal of American Ceramic Society. 2016.

[53] Tuttle B, Schwartz R. Solution deposition of ferroelectric thin films. MRS Bulletin. 1996;21(06):49–54.

[54] Schwartz RW, Reichert TL, Clem PG, Dimos D, Liu D. A comparison of diol and methanol-based chemical solution deposition routes for PZT thin film fabrication. Integrated Ferroelectrics. 1997;18(1–4):275–286.

[55] Ramamurthi SD, Payne DA. Structural investigations of prehydrolyzed precursors used in the sol-gel processing of lead titanate. Journal of the American Ceramic Society. 1990;73(8):2547–2551.

[56] Schwartz RW. Chemical solution deposition of perovskite thin films. Chemistry of Materials. 1997;9(11):2325–2340.

[57] Brinker CJ, Scherer GW. Sol → gel → glass: I. Gelation and gel structure. Journal of Non-Crystalline Solids. 1985;70(3):301–322.

[58] Esquivias L, Kallala M, Sanchez C, Cabane B. Advanced materials from gels SAXS study of gelation and precipitation in titanium-based systems. Journal of Non-Crystalline Solids. 1992;147:189–193.

[59] Brinker CJ, Scherer GW. Sol-Gel Science: The Physics and Chemistry of Sol-Gel Processing. Academic Press, Inc.; New York. 2013.

[60] Veldhuis SA, George A, Nijland M, ten Elshof JE. Concentration dependence on the shape and size of sol-gel-derived yttria-stabilized zirconia ceramic features by soft lithographic patterning. Langmuir. 2012;28(42):15111–15117.

[61] Doeuff S, Henry M, Sanchez C, Livage J. Hydrolysis of titanium alkoxides: Modification of the molecular precursor by acetic acid. Journal of Non-Crystalline Solids. 1987;89(1): 206–216.

[62] Chatry M, Henry M, Livage J. Synthesis of non-aggregated nanometric crystalline zirconia particles. Materials Research Bulletin. 1994;29(5):517–522.

[63] Courtin E, Boy P, Rouhet C, Bianchi L, Bruneton E, Poirot N, et al. Optimized sol-gel routes to synthesize yttria-stabilized zirconia thin films as solid electrolytes for solid oxide fuel cells. Chemistry of Materials. 2012;24(23):4540–4548.

[64] Joshi V, Dacruz C, Cuchiaro J, Araujo C, Zuleeg R. Analysis of C-V and I-V data of BST thin films. Integrated Ferroelectrics. 1997;14(1–4):133–140.

[65] Vest RW, Jiejie X. $PbTiO_3$/films from metalloorganic precursors. IEEE Transactions on Ultrasonics, Ferroelectrics, and Frequency Control. 1988;35(6):711–717.

[66] Cui T, Markus D, Zurn S, Polla D. Piezoelectric thin films formed by MOD on cantilever beams for micro sensors and actuators. Microsystem Technologies. 2004;10(2):137–141.

[67] Agarwal V, Liu M. Preparation of barium cerate-based thin films using a modified pechini process. Journal of Materials Science. 1997;32(3):619–625.

[68] Barrow D, Petroff T, Sayer M. Thick ceramic coatings using a sol gel based ceramic-ceramic 0–3 composite. Surface and Coatings Technology. 1995;76:113–118.

[69] Zhao H, Li X, Ju F, Pal U. Effects of particle size of 8 mol% Y_2O_3 stabilized ZrO_2 (YSZ) and additive Ta_2O_5 on the phase composition and the microstructure of sintered YSZ electrolyte. Journal of Materials Processing Technology. 2008;200(1–3):199–204.

[70] Muecke UP, Beckel D, Bernard A, Bieberle-Hütter A, Graf S, Infortuna A, et al. Micro solid oxide fuel cells on glass ceramic substrates. Advanced Functional Materials. 2008;18(20):3158–3168.

[71] Rupp JL, Drobek T, Rossi A, Gauckler LJ. Chemical analysis of spray pyrolysis gadolinia-doped ceria electrolyte thin films for solid oxide fuel cells. Chemistry of Materials. 2007;19(5):1134–1142.

[72] Rupp JL, Solenthaler C, Gasser P, Muecke U, Gauckler LJ. Crystallization of amorphous ceria solid solutions. Acta Materialia. 2007;55(10):3505–3512.

[73] Tummala R. Fundamentals of Microsystems Packaging. McGraw-Hill Professional; New York. 2001.

[74] Pan Y, Zhu J, Hu MZ, Payzant EA. Processing of YSZ thin films on dense and porous substrates. Surface and Coatings Technology. 2005;200(5):1242–1247.

[75] Lin JM, Hsu MC, Fung KZ. Deposition of ZrO_2 film by liquid phase deposition. Journal of Power Sources. 2006;159(1):49–54.

[76] Rørvik PM, Haavik C, Griesche D, Schneller T, Lenrick F, Wallenberg LR. Chemical solution deposition of thin films for protonic ceramic fuel cells. Solid State Ionics. 2014;262:852–855.

[77] Scriven L. Physics and applications of dip coating and spin coating. In: MRS Proceedings. Cambridge University Press; USA 1988.

[78] Brinker C, Frye G, Hurd A, Ashley C. Fundamentals of sol-gel dip coating. Thin Solid Films. 1991;201(1):97–108.

[79] Schunk PR, Hurd AJ, Brinker CJ, Kistler SF, Schweizer PM. Liquid film coating. In: Free-Meniscus Coating Processes. Springer; Netherland 1997. pp. 673–708.

[80] Perednis D, Gauckler LJ. Thin film deposition using spray pyrolysis. Journal of Electroceramics. 2005;14(2):103–111.

[81] Beckel D, Bieberle-Hütter A, Harvey A, Infortuna A, Muecke U, Prestat M, et al. Thin films for micro solid oxide fuel cells. Journal of Power Sources. 2007;173(1):325–345.

[82] Perednis D, Wilhelm O, Pratsinis S, Gauckler L. Morphology and deposition of thin yttria-stabilized zirconia films using spray pyrolysis. Thin Solid Films. 2005; 474(1):84–95.

[83] Somroop K, Pornprasertsuk R, Jinawath S. Fabrication of Y_2O_3-doped $BaZrO_3$ thin films by electrostatic spray deposition. Thin Solid Films. 2011;519(19):6408–6412.

[84] Perednis D, Gauckler L. Solid oxide fuel cells with electrolytes prepared via spray pyrolysis. Solid State Ionics. 2004;166(3):229–239.

[85] Takahashi Y, Matsuoka Y. Dip-coating of TiO_2 films using a sol derived from Ti(Oi-Pr)$_4$-diethanolamine-H_2O-i-PrOH system. Journal of Materials Science. 1988;23(6): 2259–2266.

[86] Haas D, Birnie D, Zecchino M, Figueroa J. The effect of radial position and spin speed on striation spacing in spin on glass coatings. Journal of Materials Science Letters. 2001;20(19):1763–1766.

[87] Bradley D, Mehrotra R, Gaur D. Metal Alkoxides. Academic Press, London; 1978.

[88] Brennecka GL, Tuttle BA. Fabrication of ultrathin film capacitors by chemical solution deposition. Journal of Materials Research. 2007;22(10):2868–2874.

[89] Tu Y, Milne S. Processing and characterization of Pb(Zr,Ti)O_3 films, up to 10 μm thick, produced from a diol sol-gel route. Journal of Materials Research. 1996;11(10):2556–2564.

[90] Brinker CJ, Clark DE, Ulrich DR. Better ceramics through chemistry II. In: MRS Symposium Proceedings. Cambridge University Press; USA. 1986.

[91] Glaser P, Pantano CG. Effect of the H_2O/TEOS ratio upon the preparation and nitridation of silica sol/gel films. Journal of Non-Crystalline Solids. 1984;63(1):209–221.

[92] Garino TJ. The cracking of sol-gel films during drying. In: MRS Proceedings. Cambridge University Press; USA. 1990.

[93] Schmidt H. Chemistry of material preparation by the sol-gel process. Journal of Non-Crystalline Solids. 1988;100(1):51–64.

[94] Schneller T, Waser R, Kosec M, Payne D. Chemical Solution Deposition of Functional Oxide Thin Films. Springer-Verlag Wien; Heidelberg. 2013.

[95] Garino TJ, Harrington M. Residual stress in PZT thin films and its effect on ferroelectric properties. In: MRS Proceedings. Cambridge University Press; USA. 1991.

[96] Chiang YM, Kingery WD, Birnie DP. Physical Ceramics: Principles for Ceramic Science and Engineering. John Wiley & Sons; New York. 1997.

[97] Schmelzer JW, Abyzov AS, Fokin VM, Schick C, Zanotto ED. Crystallization of glass-forming liquids: Maxima of nucleation, growth, and overall crystallization rates. Journal of Non-Crystalline Solids. 2015;429:24–32.

[98] Schwartz R, Voigt J, Tuttle B, Payne D, Reichert T, DaSalla R. Comments on the effects of solution precursor characteristics and thermal processing conditions on the crystal-

lization behavior of sol-gel derived lead zirconate titanate thin films. Journal of Materials Research. 1997;12(2):444–456.

[99] Keddie JL, Giannelis EP. Effect of heating rate on the sintering of titanium dioxide thin films: Competition between densification and crystallization. Journal of the American Ceramic Society. 1991;74(10):2669–2671.

IntechOpen

IntechOpen